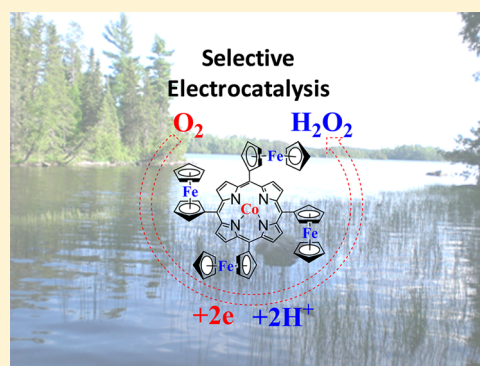


Electrochemistry and Catalytic Properties for Dioxygen Reduction Using Ferrocene-Substituted Cobalt Porphyrins

Bin Sun,[†] Zhongping Ou,^{*,†} Deying Meng,[†] Yuanyuan Fang,[‡] Yang Song,[‡] Weihua Zhu,[†] Pavlo V. Solntsev,[§] Victor N. Nemykin,^{*,§} and Karl M. Kadish^{*,‡}[†]School of Chemistry and Chemical Engineering, Jiangsu University, Zhenjiang 212013, China[‡]Department of Chemistry, University of Houston, Houston, Texas 77204-5003, United States[§]Department of Chemistry & Biochemistry, University of Minnesota Duluth, Duluth, Minnesota 55812-2496, United States

S Supporting Information

ABSTRACT: Cobalt porphyrins having 0–4 *meso*-substituted ferrocenyl groups were synthesized and examined as to their electrochemical properties in *N,N'*-dimethylformamide (DMF) containing 0.1 M tetra-*n*-butylammonium perchlorate as a supporting electrolyte. The examined compounds are represented as $(\text{Fc})_n(\text{CH}_3\text{Ph})_{4-n}\text{PorCo}$, where Por is a dianion of the substituted porphyrin, Fc and CH_3Ph represent ferrocenyl and/or *p*- $\text{CH}_3\text{C}_6\text{H}_4$ groups linked at the four *meso*-positions of the macrocycle, and *n* varies from 0 to 4. Each porphyrin undergoes two reversible one-electron reductions and two to six one-electron oxidations in DMF, with the exact number depending upon the number of Fc groups on the compound. The first electron addition is metal-centered to generate a Co(I) porphyrin. The second is porphyrin ring-centered and leads to formation of a Co(I) π -anion radical. The first oxidation of each Co(II) porphyrin is metal-centered to generate a Co(III) derivative under the given solution conditions. Each ferrocenyl substituent can also be oxidized by one electron, and this occurs at more positive potentials. Each compound was investigated as a catalyst for the electroreduction of dioxygen when adsorbed on a graphite electrode in 1.0 M HClO_4 . The number of electrons transferred (*n*) during the catalytic reduction was 2.0 for the three ferrocenyl substituted compounds, consistent with only H_2O_2 being produced as a product of the reaction. Most monomeric cobalt porphyrins exhibit *n* values between 2.6 and 3.1 under the same solution conditions, giving a mixture of H_2O and H_2O_2 as a reduction product, although some monomeric porphyrins can give an *n* value of 4.0. Our results in the current study indicate that appending ferrocene groups directly to the *meso* positions of a porphyrin macrocycle will increase the selectivity of the oxygen reduction, resulting in formation of only H_2O_2 as a reaction product. This selectivity of the electrocatalytic oxygen reduction reaction is explained on the basis of steric hindrance by the ferrocene substituents which prevent dimerization.



INTRODUCTION

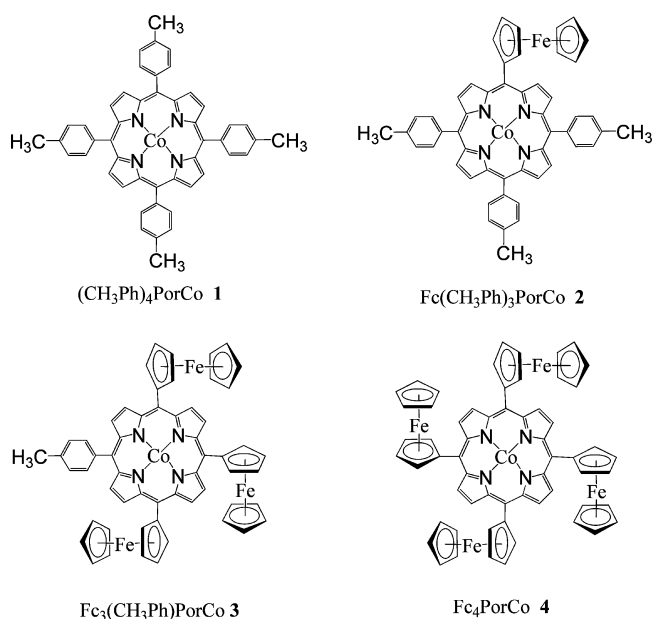
Ferrocenyl-containing compounds, such as phthalocyanines,^{1,2} tetraazaporphyrins,^{3–6} corroles,^{7–9} and especially porphyrins^{10–41} have received considerable attention, in part because of their rich redox activity which is of fundamental importance for the development of molecular-based electronic devices^{42–45} or molecular electrogenic sensors.⁴⁶ The ability of these types of compounds to reversibly accept and/or release multiple electrons at distinct potentials is particularly important in the area of multielectron redox catalysis⁴⁷ and information storage at the molecular level.^{48,49}

The addition of one or more electron-donating or electron-withdrawing substituents onto the *meso*- or β -pyrrole positions of a porphyrin, corrole, or related macrocycle will have a significant effect on the compound's UV–visible spectra and redox potentials.⁵⁰ This is also the case when ferrocene groups are connected to the *meso* positions of a porphyrin macrocycle.^{13–19,28,51,52}

The well-known electron-donor properties of ferrocene have been effectively utilized to enhance the catalytic activity of cobalt^{53,54} and copper^{55–57} complexes in the electrocatalytic four-electron reduction of oxygen to water. It has been reported that an iron porphyrin linked to four ferrocene groups with short conjugated spacers in an $\alpha_4\text{-FeFc}_4$ arrangement can also catalyze the four-electron reduction of O_2 to H_2O .²⁷ However, it was not known if a similar enhancement of the catalyst might occur when Fc groups are *directly* connected at the *meso* position of a porphyrin. This is investigated in the present paper where we have characterized four Co(II) porphyrins having zero, one, three, and four ferrocenyl groups directly connected on the *meso* positions of the macrocycle. The structures of the examined cobalt compounds are shown in Chart 1.

Received: May 23, 2014

Published: July 28, 2014

Chart 1. Structures of Examined *meso*-Substituted Cobalt(II) Porphyrins

It has been demonstrated that monomeric cobalt porphyrins, when adsorbed on a carbon electrode, can catalyze two- or four-electron reduction of O₂ in an acid media with the formation of a H₂O₂ and/or H₂O product. The catalytic activity and selectivity of the cobalt porphyrins (i.e., two- versus four-electron pathways) should be dependent on the type and location of the macrocycle substituents as well as on the planarity of the macrocycle.^{58,59} In the present study, the catalytic activity of the compounds in Chart 1 toward the reduction of molecular oxygen was evaluated in acid media by utilizing cyclic voltammetry and linear sweep voltammetry with a rotating disk electrode (RDE) and a rotating ring-disk electrode (RRDE). The effect of the ferrocenyl groups on the UV–visible spectra, reduction/oxidation potentials, and the catalytic activity of the currently examined compounds are reported with comparisons made to nonferrocenyl substituted cobalt porphyrins previously examined under similar experimental conditions.

EXPERIMENTAL SECTION

Instrumentation. Thin-layer UV–visible spectroelectrochemical experiments were performed with a home-built thin-layer cell which has a light transparent platinum net working electrode. Potentials were applied and monitored with an EG&G PAR Model 173 potentiostat. Time-resolved UV–visible spectra were recorded with a Hewlett-Packard Model 8453 diode array spectrophotometer. High purity N₂ was used to deoxygenate the solution and kept over the solution during each electrochemical and spectroelectrochemical experiment.

Cyclic voltammetry was carried out at 298 K by using an EG&G Princeton Applied Research (PAR) 173 potentiostat/galvanostat or CHI-730C Electrochemical Workstation. A homemade three-electrode cell was used for all electrochemical measurements. A three-electrode system was used in each case and consisted of a glassy carbon or graphite working electrode (Model MT134, Pine Instrument Co.) for cyclic voltammetry and voltammetry at an RDE and a platinum-ring, graphite-disk electrode combination for voltammetry at the RRDE. A platinum wire served as the auxiliary electrode and a saturated calomel electrode (SCE) as the reference electrode, which was separated from the bulk of the solution by a salt bridge of low porosity which contained the solvent/supporting electrolyte mixture. The rotating

ring-disk electrode (RRDE) was purchased from Pine Instrument Co. and consisted of a platinum ring and a removable edge-plane pyrolytic graphite (EPPG) disk ($A = 0.196 \text{ cm}^2$). A Pine Instrument MSR speed controller was used for the RDE and RRDE experiments. The Pt ring was first polished with $0.05 \mu\text{m}$ α -alumina powder and then rinsed successively with water and acetone before being activated by cycling the potential between 1.20 and -0.20 V in 1.0 M HClO_4 until reproducible voltammograms were obtained.^{60,61}

The catalysts were irreversibly adsorbed on the electrode surface by a dip-coating procedure described in the literature.^{62,63} The freshly polished electrode was dipped in a 1.0 mM catalyst solution of CH₂Cl₂ for 5 s, transferred rapidly to pure CH₂Cl₂ for 1–2 s, and then exposed to air where the adhering solvent rapidly evaporated, leaving the porphyrin catalyst adsorbed on the electrode surface. All experiments were carried out under room temperature. The average number of electrons transferred (n) and the amount of H₂O₂ formed in the catalytic reduction of O₂ were determined by the Koutecky–Levich plots⁶⁴ and calculated with eqs 1 and 2.

$$n = 4I_D / (I_D + I_R/N) \quad (1)$$

$$\% \text{H}_2\text{O}_2 = 100(2I_R/N) / (I_D + I_R/N) \quad (2)$$

where I_D and I_R are the Faradaic currents at the disk and ring electrodes, respectively. The intrinsic value of the collection efficiency (N) was determined to be 0.24 using the $[\text{Fe}(\text{CN})_6]^{3-}/[\text{Fe}(\text{CN})_6]^{4-}$ redox couple in 1.0 M KCl .

Chemicals. Reagents and solvents (Sigma-Aldrich, Fluka or Sinopharm Chemical Reagent Co.) for synthesis and purification were of analytical grade and used as received. Dichloromethane (CH₂Cl₂, 99.8%) was purchased from EMD Chemicals Inc. and used as received. Tetra-*n*-butylammonium perchlorate (TBAP) was purchased from Sigma Chemical or Fluka Chemika Co., recrystallized from ethyl alcohol, and dried under a vacuum at $40 \text{ }^\circ\text{C}$ for at least 1 week prior to use.

The examined compounds are represented as $(\text{Fc})_n(\text{CH}_3\text{Ph})_{4-n}\text{PorCo}$, where Por is a dianion of the substituted porphyrin, Fc and CH₃Ph represent ferrocenyl and/or *p*-CH₃C₆H₄ groups linked at the four *meso* positions of the macrocycle, and n varies from 0 to 4. Details on the synthesis and properties of the investigated porphyrins are given below.

(CH₃Ph)₄PorCo, 1. This compound was synthesized according to a procedure described in the literature.⁶⁵

Fc(CH₃Ph)₃PorCo, 2. A mixture of the free-base porphyrin, Fc(CH₃Ph)₃PorH₂⁵¹ (30 mg, 0.036 mmol), and cobalt acetate tetrahydrate (30 mg, 0.12 mmol) in 20 mL of DMF was heated for 4 h at $140 \text{ }^\circ\text{C}$. The solvent was removed when the reaction was complete, and the residue was then dissolved in CH₂Cl₂ and subjected to chromatography on silica-gel using a mixed solvent of CH₂Cl₂/*n*-hexane = 1:1 as an eluent. The brown-red solution was collected and the solvent evaporated to dryness at $40\text{--}50 \text{ }^\circ\text{C}$ for 12 h. Yield: 60%. UV–vis ($\lambda_{\text{max}}/\text{nm}$, CH₂Cl₂): 412, 532. Elem. Anal. Calcd for C₅₁H₃₈N₄FeCo: C, 74.55; H, 4.66; N, 6.82%. Found: C, 74.36; H, 4.52; N, 6.79%. MS: m/z 821.18. Calcd. $[\text{M} - \text{H}]^+$: 821.17.

Fc₃(CH₃Ph)PorCo, 3. A mixture of the free-base porphyrin, Fc₃(CH₃Ph)PorH₂⁵¹ (30 mg, 0.04 mmol), and cobalt acetate tetrahydrate (25 mg, 0.10 mmol) in 20 mL of DMF was heated 6 h at $140 \text{ }^\circ\text{C}$. The solvent was removed when the reaction was complete, and the residue was then dissolved in CH₂Cl₂ and subjected to chromatography on silica-gel using a mixed solvent of CH₂Cl₂/*n*-hexane = 1:2 as an eluent. The brown-red solution was collected and the solvent evaporated to dryness at $40\text{--}50 \text{ }^\circ\text{C}$ for 12 h. Yield: 50%. UV–vis ($\lambda_{\text{max}}/\text{nm}$, CH₂Cl₂): 414, 538. MS: m/z 1009.68. Calcd. for C₅₇H₄₅N₄Fe₃Co $[\text{M} - 2\text{H}]^+$: 1010.08.

Fc₄PorCo, 4. This porphyrin was synthesized according to a procedure described in the literature.^{15,18}

RESULTS AND DISCUSSION

Electrochemistry and Spectroelectrochemistry. Each cobalt porphyrin undergoes two reversible one-electron

reductions as seen in Figure 1. The first is located at $E_{1/2}$ values between -0.81 and -0.92 V and the second at $E_{1/2}$ between

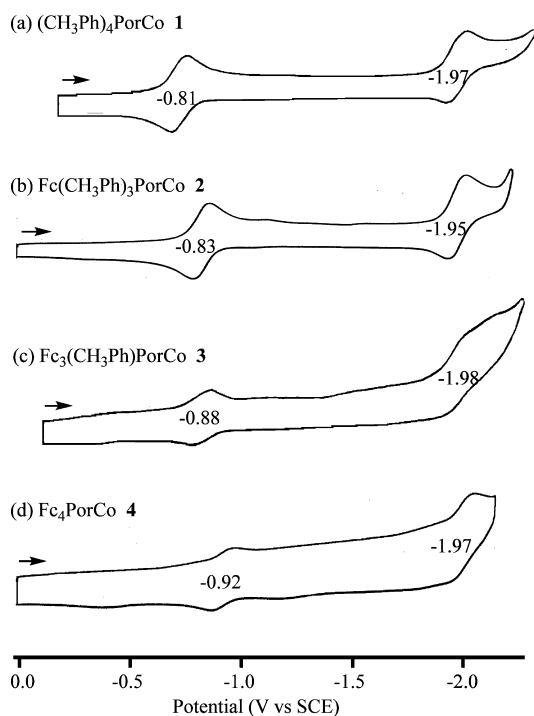


Figure 1. Cyclic voltammograms showing reductions of (a) $(\text{CH}_3\text{Ph})_4\text{PorCo}^{\text{II}}$, **1**; (b) $\text{Fc}(\text{CH}_3\text{Ph})_3\text{PorCo}^{\text{II}}$, **2**; (c) $\text{Fc}_3(\text{CH}_3\text{Ph})\text{PorCo}^{\text{II}}$, **3**; and (d) $\text{Fc}_4\text{PorCo}^{\text{II}}$, **4**, in DMF containing 0.1 M TBAP. Scan rate = 0.10 V/s.

-1.95 and -1.98 V vs SCE. Similar redox behavior has been reported for other structurally related cobalt(II) porphyrins in nonaqueous media.⁵⁰

Thin-layer UV–visible spectroelectrochemistry was utilized to elucidate the site of electron transfer, and examples of the spectral changes which occurred during controlled potential

reduction of **1** and **3** are shown in Figure 2. As the first one-electron reduction proceeds at a controlled potential of -1.00 V, the intensity of the Soret band at 416 nm (cpd **1**) or 420 nm (cpd **3**) decreases in intensity, and a new split Soret band appears at 365 and 426 nm for **1** and 376 and 450 nm for **3**. Both sets of spectral changes are consistent with an initial reduction at the central metal ion to give a Co(I) porphyrin product⁶⁶ rather than a Co(II) π -anion radical. The second controlled potential reduction at -2.20 V gives a product which is then assigned to a Co(I) porphyrin π -anion radical. Similar spectral changes are observed for compounds **2** and **4**, and these are also consistent with the stepwise generation of a Co(I) porphyrin and a Co(I) porphyrin π -anion radical.

Each linked Fc group on **2**, **3**, and **4** can be reversibly oxidized by one electron,^{15,18} and it was necessary to determine which redox process comes first upon scanning the potential in a positive direction—oxidation of the porphyrin macrocycle, oxidation of the central metal ion, or oxidation of the linked ferrocene group(s). The site of electron transfer for these oxidations was determined both by comparison with literature data for the oxidation of similar cobalt porphyrins⁵⁰ and confirmed as well as by the spectroelectrochemistry described as follows in this article.

The first oxidation of each cobalt(II) porphyrin involves an irreversible $\text{Co}^{\text{II}}/\text{Co}^{\text{III}}$ process at a scan rate of 0.1 V/s. These processes are located at $E_{\text{pa}} = 0.45$ V for **1**, 0.30 V for **2**, 0.25 V for **3**, and 0.15 V for **4** in DMF containing 0.10 M TBAP (see Figure 3 and Table 1). The reverse $\text{Co}^{\text{III}}/\text{Co}^{\text{II}}$ rereduction process is also irreversible at a scan rate of 0.1 V/s and occurs at more negative potentials of -0.08 , -0.22 , $+0.02$, and -0.37 V for compounds **1–4**.

It is known that the neutral Co(II) porphyrins can axially bind one DMF solvent molecule to form five-coordinate complexes while Co(III) porphyrins will strongly bind two DMF molecules and are six coordinate.⁵⁰ The irreversibility of the $\text{Co}^{\text{II}}/\text{Co}^{\text{III}}$ process is known to occur in all coordinating solvents (such as DMF), and this is due to a change of coordination number from 5 to 6 upon electron transfer. The combined oxidation and rereduction mechanism for this

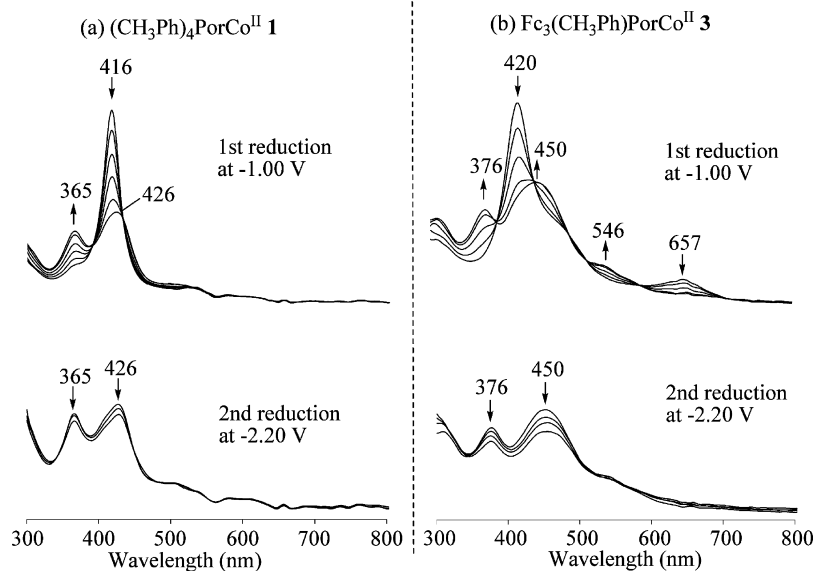


Figure 2. Thin-layer UV–visible spectral changes of (a) $(\text{CH}_3\text{Ph})_4\text{PorCo}^{\text{II}}$, **1**, and (b) $\text{Fc}_3(\text{CH}_3\text{Ph})\text{PorCo}^{\text{II}}$, **3**, during the controlled potential reductions in DMF containing 0.1 M TBAP.

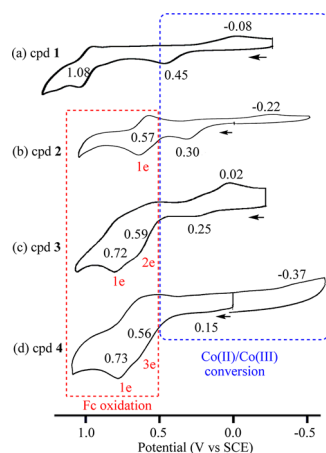


Figure 3. Cyclic voltammograms showing oxidations of (a) $(\text{CH}_3\text{Ph})_4\text{PorCo}^{\text{II}}$, **1**; (b) $\text{Fc}(\text{CH}_3\text{Ph})_3\text{PorCo}^{\text{II}}$, **2**; (c) $\text{Fc}_3(\text{CH}_3\text{Ph})\text{PorCo}^{\text{II}}$, **3**; and (d) $\text{Fc}_4\text{PorCo}^{\text{II}}$, **4**, in DMF containing 0.1 M TBAP. Scan rate = 0.10 V/s.

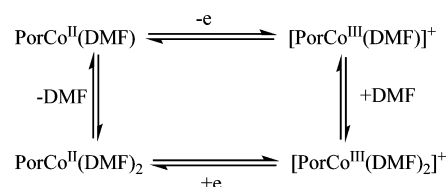
process has previously been elucidated⁵⁰ and is shown by the “square mechanism” in Scheme 1.

The site of electron transfers in the first oxidation of compounds **1–4** was confirmed by *in situ* thin-layer UV–visible spectroelectrochemical measurements. As seen in Figure 4a, the original Soret band of the neutral Co(II) porphyrin at 416 nm decreases in intensity, and a new sharp Soret band for Co(III) grows at 432 nm during the first one-electron oxidation of compound **1** at an applied potential of 0.60 V. Similar Co(III) spectra are observed after the first oxidation of the ferrocenyl substituted compounds **2**, **3** (Figure 4b,c), and **4** (Figure S1), although the direction of λ_{max} shifts from 432 nm of **1** to 448 nm of **4** due to the effect of the electron-donating ferrocene group (see Table 2).

In the case of compound **1**, which lacks an Fc group, only metal and porphyrin ring-centered oxidations are possible, and the macrocycle-centered process occurs at 1.08 V in DMF (see Figure 3a). This is consistent with the UV–visible data in Figure 4a, which show a loss of the Soret band intensity as a Co(III) π -cation radical is generated upon abstraction of a second electron from compound **1**.

The oxidation potential of the parent ferrocene in DMF containing the 0.1 M TBAP system is 0.50 V, and similar oxidation potentials are observed at 0.56–0.59 V for compounds **2**, **3**, and **4** (Figure 3b–d). Additional oxidations are observed at 0.72 V for **3** and 0.73 V for **4** (Figure 3c,d). These later processes at more positive potentials are all proposed to occur on the *meso*-linked Fc groups. Thus, two different oxidation routes can be proposed for the second oxidation of **1–4** as shown in Scheme 2.

Scheme 1. Proposed Mechanism for the First Oxidation of Compounds **1–4** in DMF



It should be noted that the potentials for oxidation of the ferrocenyl group on the porphyrins **2–4** are shifted positively by 60–230 mV as compared to the potential for oxidation of free ferrocene ($E_{1/2} = 0.50$ V) while at the same time the Co^{II}/Co^{III} process of **2–4** is negatively shifted by 150–300 mV under the same solution conditions. This indicates that an interaction occurs between the electroactive ferrocenyl substituent(s) which become(s) harder to oxidize and the electroactive porphyrin macrocycle which becomes easier to oxidize as compared to compound **1** which lacks a Fc group. An interaction also occurs between the multiple ferrocenyl groups on compounds **3** and **4** which are nonequivalent as demonstrated by the different redox potentials for the Fc groups in the two porphyrins (see Figure 3 and Table 1). It should be noted that the degree of metal–metal coupling in compounds **3** and **4** is smaller than that for the bis(ferrocenyl)-containing porphyrins reported by Officer and co-workers⁶⁷ but larger than that of the ferrocenyl-containing iron porphyrins examined by Dey and co-workers, who did not observe any metal–metal coupling.⁶⁸

Consistent with the different sites of electron transfer, significant differences are seen in the spectral changes which occur during the second oxidation of the nonferrocenyl substituted compound **1** and the ferrocenyl substituted compounds **2–4**. As shown in Figure 4a, the Soret band at 432 nm of the Co(III) porphyrin for **1** decreases significantly in intensity during controlled potential oxidation at 1.30 V, while only minimal spectral changes are seen for the second oxidation of the ferrocenyl substituted compounds **2–4** where the conjugated π -system of the porphyrin macrocycle remains unchanged (see Figure 4b and c for spectral changes of compounds **2** and **3**).

Electrocatalytic Reduction of O₂. Electroreduction of each cobalt porphyrin was carried out in 1.0 M HClO₄ saturated with N₂ or air using an EPPG disk where the porphyrin catalyst was adsorbed on the surface of the electrode. Examples of the cyclic voltammograms obtained for compounds **1**, **2**, and **3** under N₂ or air are illustrated in Figure 5.

The cyclic voltammograms under N₂ are characterized by an Co(III)/Co(II) reduction peak at $E_{\text{pc}} = 0.07$ V (**1**), 0.20 V (**2**), and 0.14 V (**3**) at a scan rate of 50 mV/s, but when the solution

Table 1. Half-Wave Potentials (V vs SCE) of the Cobalt Porphyrins **1–4** in DMF, 0.1 M TBAP

compound	oxidation			reduction	
	ring-centered	Fc-centered	Co ^{II} /Co ^{III} ^a	Co ^{II} /Co ^I	ring-centered
$(\text{CH}_3\text{Ph})_4\text{PorCo}$, 1	1.08		0.45	−0.81	−1.97
$\text{Fc}(\text{CH}_3\text{Ph})_3\text{PorCo}$, 2	1.13 ^a	0.57	0.30	−0.83	−1.95
$\text{Fc}_3(\text{CH}_3\text{Ph})\text{PorCo}$, 3	1.25	0.72	0.59 ^b	−0.88	−1.98
Fc_4PorCo , 4		0.73	0.56 ^c	−0.92	−1.97

^aIrreversible peak potential at a scan rate of 0.10 V/s. ^bTwo overlapping one-electron oxidation processes. ^cThree overlapping one-electron oxidation processes.

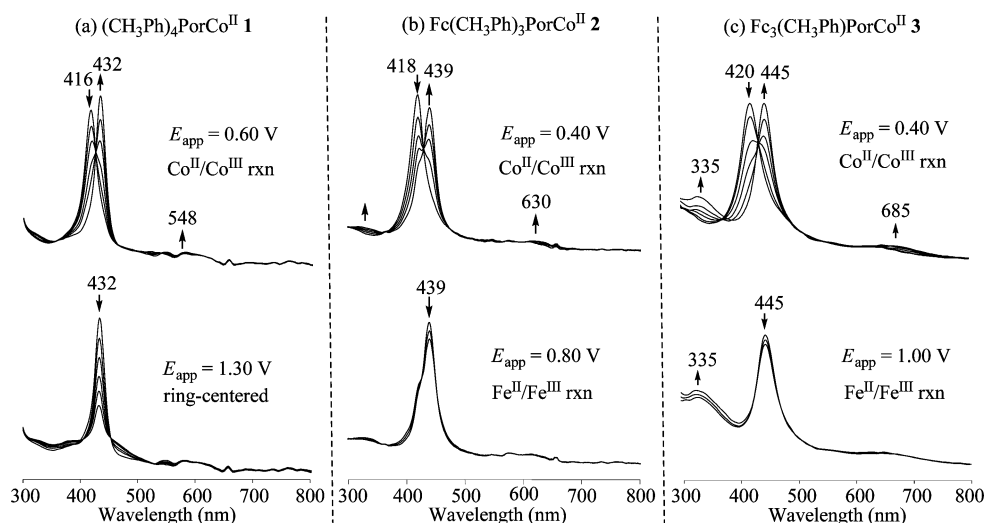
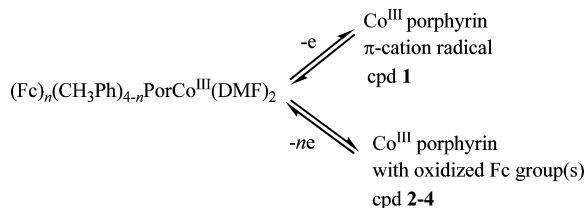


Figure 4. UV–visible spectral changes of (a) $(\text{CH}_3\text{Ph})_3\text{PorCo}^{\text{II}}$, **1**; (b) $\text{Fc}(\text{CH}_3\text{Ph})_3\text{PorCo}^{\text{II}}$, **2**; and (c) $\text{Fc}_3(\text{CH}_3\text{Ph})\text{PorCo}^{\text{II}}$, **3**, during the controlled potential oxidations in DMF containing 0.1 M TBAP.

Table 2. UV–Visible Spectral Data (λ_{max} , nm) and the Corresponding Energy (eV) of the Bands for Compounds 1–4 in DMF

compound	Soret band (nm)		E (eV)	
	Co(II)	Co(III)	Co(II)	Co(III)
$(\text{CH}_3\text{Ph})_4\text{PorCo}$, 1	416	432	2.9827	2.8720
$\text{Fc}(\text{CH}_3\text{Ph})_3\text{PorCo}$, 2	418	439	2.9685	2.8262
$\text{Fc}_3(\text{CH}_3\text{Ph})\text{PorCo}$, 3	420	445	2.9543	2.7881
Fc_4PorCo , 4	421	448	2.9473	2.7694

Scheme 2. Proposed Mechanism of the Second Oxidation of Compounds 1–4



is saturated with air, the peak potential shifts to $E_{\text{pc}} = 0.05$ V (**1**), 0.19 V (**2**), and 0.13 V (**3**) and the cathodic peak current becomes larger (see Figure 5). The large increase in peak current under air combined with the lack of a reverse anodic peak on the cyclic voltammograms is characteristic of a catalytic process, which in this case would be the catalytic reduction of O_2 to generate H_2O_2 and/or H_2O at the surface of the EPPG disk electrode.

The cyclic voltammogram obtained at a bare EPPG electrode under N_2 or air exhibits a reversible surface peak at ~ 0.40 V (Figure 6a). This surface process is labeled by an asterisk and was previously characterized in the literature as due to oxidation of the carbon electrode.^{69–71} A surface process at ~ 0.40 V is also seen at an EPPG electrode coated with ferrocene (Figure 6b), but a second reversible process is seen at +0.17 V and is assigned to the surface oxidation of ferrocene.

The potential and currents for the surface FcH^+/FcH process of ferrocene are the same under air and under N_2 (Figure 6b). The value of $E_{1/2}$ at the surface is 0.17 V and a similar $E_{1/2}$ of 0.14 V is seen for the solution oxidation/reduction of ferrocene

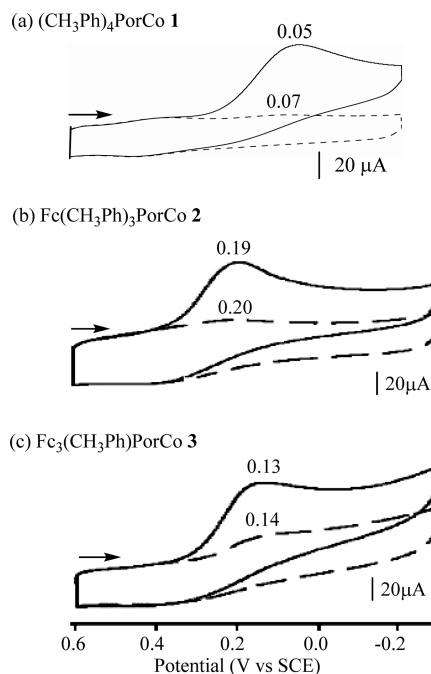


Figure 5. Cyclic voltammograms of cobalt porphyrins **1**, **2**, and **3** adsorbed on an EPPG electrode in 1.0 M HClO_4 saturated with N_2 (----) or with air (—). Scan rate = 50 mV/s.

in HClO_4 (Figure 6c). No increase in the currents for the FcH^+/FcH process are seen upon going from N_2 to air as the gas above the solution, and this indicates that ferrocene is not involved in the catalytic reduction of molecular oxygen. This result is also consistent with what has been reported for other ferrocenyl substituted metalloporphyrins.⁶⁸

Linear sweep voltammetry of each cobalt porphyrin was carried out in air-saturated 1.0 M HClO_4 in order to determine the electrocatalytic activity of the four target cobalt complexes. The numbers of electrons transferred in the reduction were then determined from the magnitude of the steady-state limiting currents that were taken at a fixed potential (-0.10 V) on the catalytic wave plateau of the current–voltage curve.

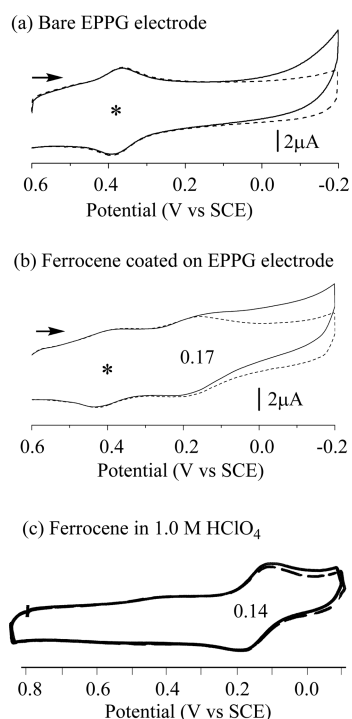


Figure 6. Cyclic voltammograms of (a) bare EPPG electrode only, (b) ferrocene adsorbed on an EPPG electrode in 1.0 M HClO₄, and (c) ferrocene in 1.0 M HClO₄ solution saturated with N₂ (-----) or with air (—). Scan rate of 50 mV/s for a and c, and 100 mV for b. * = surface process due to carbon oxidation.

Representative current–voltage curves obtained for compounds 2–4 are presented in Figure 7 and Figure S2a. The diagnostic Koutecky–Levich plots⁶⁴ are also illustrated in these figures, and the slope of a plot obtained by linear regression was then used to estimate the average number of electrons (n) involved in the catalytic reduction of O₂.

The Koutecky–Levich plots are interpreted on the basis of eq 3, where j_{lim} is the measured limiting current density (mA·cm⁻²), j_{k} is the kinetic current, and j_{lev} is the Levich current which is used to measure the rate of the current-limiting chemical reaction as defined by eq 4.

$$1/j_{\text{lim}} = 1/j_{\text{lev}} + 1/j_{\text{k}} \quad (3)$$

$$j_{\text{lev}} = 0.62nFD^{2/3}cv^{-1/6}\omega^{1/2} \quad (4)$$

The value of n in eq 4 is the number of electrons transferred in the overall electrode reaction, F is the Faraday constant (96485 C·mol⁻¹), D and c are the diffusion coefficient (cm²/s) and bulk concentration of O₂ (mol/L) in 1.0 M HClO₄, ν is the kinematic viscosity of water, and ω is the angular rotation speed (rad/s) of the electrode.

The calculated number of electrons transferred (n) to O₂ in the electroreduction process using compounds 1–4 as catalysts and the corresponding percentage of the H₂O₂ product are given in Table 3. A two electron transfer ($n = 2$) would generate 100% H₂O₂ while a four electron transfer ($n = 4$) would give 0% H₂O₂ and 100% H₂O. The Koutecky–Levich plots in Figures 7 and S2b showed that the number of electrons transferred (n) for compounds 2, 3, and 4 to be 2.1, 2.0, and 2.1, which corresponds to 95–100% H₂O₂ produced (Table 3), indicating that the catalytic electroreduction of O₂ by 2, 3, and

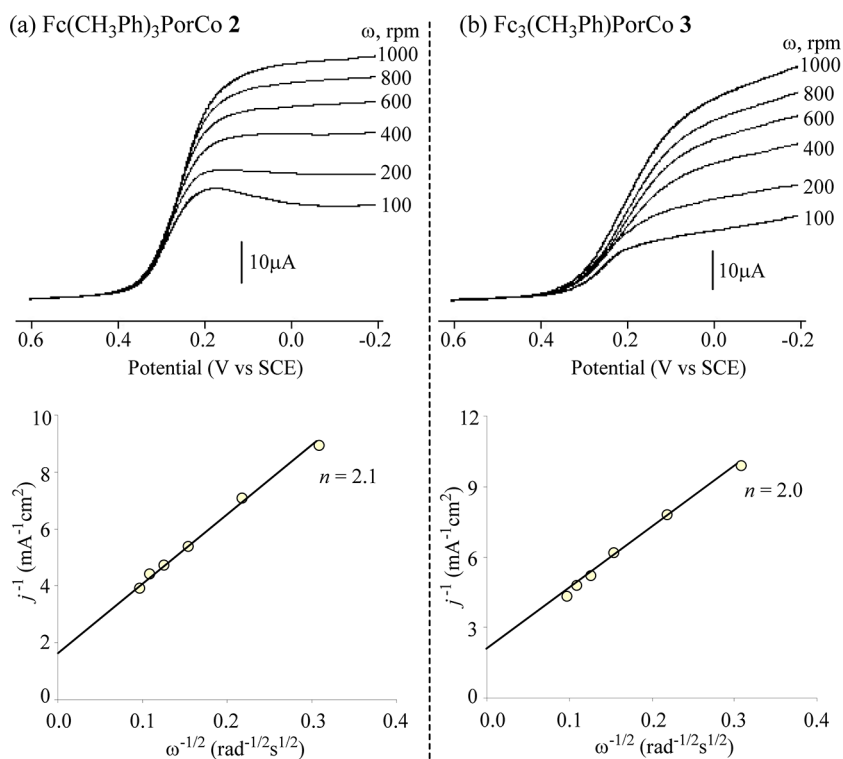


Figure 7. Current–voltage curves and Koutecky–Levich plots for catalyzed reduction of O₂ at a rotating EPPG disk electrode coated with the cobalt porphyrins 2 and 3 in 1.0 M HClO₄ saturated with air. Values of the electrode rotation rates (ω) are indicated on each curve. Potential scan rate = 50 mV/s.

Table 3. Peak Potentials (V vs SCE) of Cobalt(II) Porphyrins for Catalytic Reduction of O₂ in 1.0 M HClO₄, the Number of Electron Transferred (*n*), and the Amount of H₂O₂ Produced during the Reaction

catalyst	<i>E</i> _{pc} without O ₂	<i>E</i> _{pc} with O ₂	<i>n</i>	H ₂ O ₂ %
(CH ₃ Ph) ₄ PorCo, 1	0.07	0.05	2.8	60
Fc(CH ₃ Ph) ₃ PorCo, 2	0.20	0.19	2.1	95
Fc ₃ (CH ₃ Ph)PorCo, 3	0.14	0.13	2.0	100
Fc ₄ PorCo, 4	0.30	0.29	2.1	95

4 is mainly a 2e⁻ transfer process, giving almost exclusively H₂O₂ rather than a 4e⁻ transfer process to produce H₂O.

The catalytic reduction of O₂ was also examined at an RRDE under the same solution conditions, and examples of the relevant current–voltage curves are shown in Figure 8 for

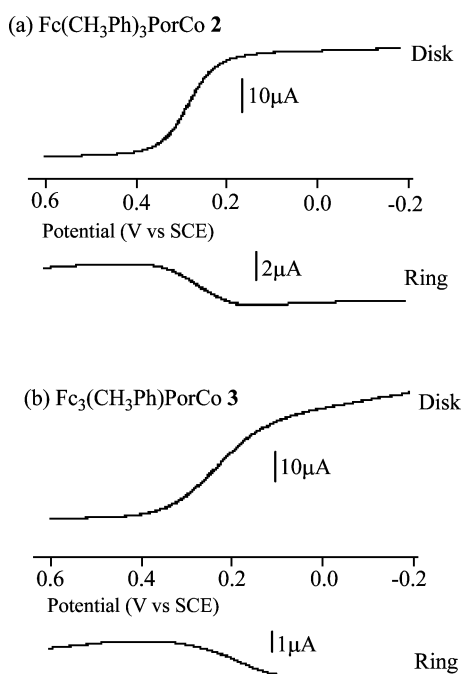


Figure 8. Rotating ring-disk electrode voltammograms of cobalt porphyrins 2 and 3 in 1.0 M HClO₄ saturated with air. The potential of the disk electrode was scanned in a negative direction from 0.6 V to -0.2 V while the potential of the ring electrode was held at 1.0 V. Rotation rate = 400 rpm and scan rate = 10 mV/s.

compounds 2 and 3. The disk potential was scanned from 0.6 to -0.2 V at a rotation speed of 400 rpm while holding the ring potential constant at 1.0 V. As seen in the figure, the disk current begins to increase at about 0.40 V for compounds 2 and 0.30 V for 3, and a plateau is reached at about 0.20 V for 2 and 0.15 V for 3. The anodic ring current increases throughout the range of the disk potentials where the disk current rises. From the Faradaic currents at the disk (*I*_D) and at the ring (*I*_R), the amount of H₂O₂ generated upon the reduction of dioxygen was calculated using eq 2 as 88% and 92% for compounds 2 and 3, respectively, under the given experimental conditions. These values are smaller than those calculated using the Koutecky–Levich plots in Figure 7.

Effect of Ferrocenyl Substituents on Spectra and Redox Potentials. A linear relationship exists between the energy of the Soret band for the Co(II) and Co(III) porphyrins and the number of ferrocenyl groups on compounds 1–4. The

measured wavelengths in nanometers and the calculated values of energy in electronvolts are given in Table 2, and a plot of Soret band energy vs number of Fc groups is shown in Figure 9a. From this figure, it is clear that the Soret band undergoes a

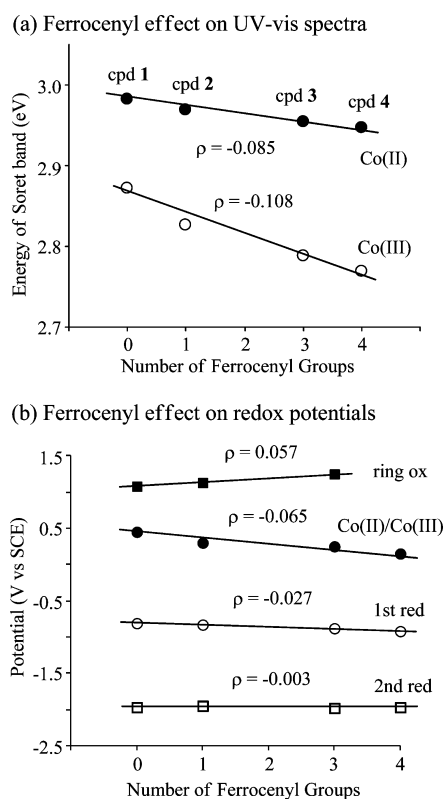


Figure 9. Plots of number of ferrocenyl groups of the porphyrin vs (a) energy of the Soret band of Co(II) and Co(III) porphyrins and (b) redox potentials of the porphyrin ring-centered and metal-centered electron transfer.

low-energy shift as the number of Fc groups is increased from 0 to 4. The slope of the plot of Soret band energy vs the number of Fc is -0.085 for Co(II) and -0.108 for Co(III). Thus, the Co(III) porphyrins are slightly more sensitive to the electron-donating Fc groups than the Co(II) porphyrins.

Linear relationships are also seen between the measured redox potentials and the number of ferrocenyl groups on compounds 1–4. The largest substituent effect is seen for the Co^{II}/Co^{III} process and the smallest for the second reduction, which is almost totally insensitive to the electron-donating substituent. The first oxidation potential shifts negatively by 300 mV upon going from compound 1 (*E*_{pa} = 0.45 V) to compound 4 (*E*_{pa} = 0.15 V), and the slope of the plot in Figure 9b shows an average shift in peak potential for the Co^{II}/Co^{III} process of about 65 mV per added Fc group on the compound. The first reduction of the Co(II) porphyrins shifts negatively by an average of 27 mV per added Fc group on the compounds, while the second reduction has a slope of almost zero as seen in Figure 9b. In contrast, the porphyrin ring-centered oxidation shifts positively with an increase in the number of linked Fc groups, but it should be noted that the overall charge on the electroactive species is different in each case, being +1 in the case of 1, +2 in the case of 2, and +4 in the case of compound 3 where the three Fc groups have been oxidized. Thus, the harder oxidation of the porphyrin ring upon going from compound 1

Table 4. Number of Electron Transferred (n) for Catalytic Reduction of O_2 by Different Cobalt Porphyrins Used as Catalyst in Acid Media^a

catalyst	β -group	<i>meso</i> -group	n	acid media	ref
(CH ₃) ₄ PorCo	none	CH ₃	4.0	1.0 M HClO ₄	63
(Por)Co	none	none	4.0	1.0 M HClO ₄	73
NO ₂ (CH ₃ Ph) ₄ PorCo	NO ₂	CH ₃ Ph	3.1	1.0 M HClO ₄	58
NO ₂ (3,5-diCH ₃ OPh) ₄ PorCo	NO ₂	CH ₃ OPh	3.1	1.0 M HClO ₄	58
(OEP)Co	C ₂ H ₅	none	2.8		59
(CH ₃ Ph) ₄ PorCo	none	CH ₃ Ph	2.8	1.0 M HClO ₄	<i>tw</i>
(3,5-diCH ₃ OPh) ₄ PorCo	none	CH ₃ OPh	2.6	1.0 M HClO ₄	58
(PPIX)Co	CH ₃ , CHCH ₂ , C ₂ H ₄ COOH	none	2.6	1.0 M HClO ₄	59
(TPP)Co	none	Ph	2.0	1.0 M HClO ₄	59, 63
(TPyP)Co	none	Py	2.0	0.05 M H ₂ SO ₄	59, 74
Fc(CH ₃ Ph) ₃ PorCo	none	Fc, CH ₃ Ph	2.1	1.0 M HClO ₄	<i>tw</i>
Fc ₃ (CH ₃ Ph)PorCo	none	Fc, CH ₃ Ph	2.0	1.0 M HClO ₄	<i>tw</i>
Fc ₄ PorCo	none	Fc, CH ₃ Ph	2.1	1.0 M HClO ₄	<i>tw</i>

^a*tw* = this work.

to compound **4** may be due to the increased positive charge on the compound rather than to the effect of increasing the number of Fc groups.

Effect of Ferrocenyl Groups on the Catalytic Electroreduction of Dioxygen. As discussed above, free ferrocene shows no catalytic activity for the reduction of O_2 in acid media. However, ferrocene substituents in complexes **2–4** also have no effect on the four-electron electrocatalytic activity of the target cobalt porphyrins, although it should be noted that adding ferrocene groups directly to the *meso* positions of the porphyrin will change the planarity of the porphyrin macrocycle.¹⁵ The steric hindrance resulting from addition of these groups at the *meso* positions of the macrocycle will also prevent the formation of dimers on the electrode surface, thus preventing the occurrence of a four-electron reduction to give an H_2O reduction product and an n value of 4.⁶³

We have previously reported that the electroreduction of O_2 catalyzed by triphenylcorroles which contain substituents on the *ortho* positions of the *meso*-phenyl rings give, in most cases, a two-electron transfer process ($n = 2$) and only H_2O_2 as the product. This is because *ortho* positions of the *meso*-phenyl rings of the triphenyl corrole can lead to steric hindrance and block the π - π interaction of the macrocycles.⁷²

It is also known that the catalytic activity of the monomeric cobalt porphyrins will depend not only on the nature of the substituents but also on steric interactions involving bulky substituents on the *meso*-phenyl rings. As can be seen from Table 4, cobalt porphine and cobalt tetramethylporphyrin, (CH₃)₄PorCo, which lack bulky *meso* substituents, will both catalyze the reduction of O_2 via a four-electron pathway ($n = 4$) to give H_2O as a final product.^{63,73} The reason for such selectivity is the formation of porphyrin dimers, which can carry out the four-electron electrocatalytic reduction of dioxygen. (TPP)Co and (TPyP)Co can only catalyze a two-electron reduction of dioxygen ($n = 2$),^{59,63,74} while the values of n range from 2.6 to 3.1 when other substituted monocobalt porphyrins were utilized as the catalysts.^{58,59} The values of $n = 2$ for the current investigated ferrocene substituted compounds are consistent with a steric hindrance of ferrocene substituents, which prevent formation of porphyrin dimers. Thus, the cobalt *meso*-ferrocenyl porphyrins discussed in this paper can be proposed as selective electrocatalysts for two-electron reduction of oxygen.

CONCLUSION

Several cobalt *meso*-ferrocenyl porphyrins of general formula $Fc_n(CH_3Ph)_{4-n}PorCo$ ($n = 0-4$) with direct ferrocene-to-porphyrin bonds have been prepared and investigated using UV-vis spectroscopy as well as electrochemical and spectroelectrochemical approaches. The electron-donating ferrocene substituent(s) have a significant effect on the compound's UV-visible spectra as well as on their cobalt-centered and porphyrin ring-centered redox potentials. The electrocatalytic properties of the investigated ferrocenyl-containing cobalt porphyrins are highly selective in the electrocatalytic reduction of dioxygen and lead almost exclusively to formation of hydrogen peroxide as a reaction product. Such a high selectivity can be explained on the basis of steric hindrance resulting from the bulky ferrocene groups which prevents dimerization of the porphyrin on the electrode surface.

ASSOCIATED CONTENT

Supporting Information

Spectroelectrochemistry, current-voltage curves, and Koutecky-Levich plot of Fc_4PorCo in 1.0 M HClO₄ saturated with air. This material is available free of charge via the Internet at <http://pubs.acs.org>.

AUTHOR INFORMATION

Corresponding Authors

*E-mail: zpou2003@yahoo.com.

*E-mail: vnemykin@d.umn.edu.

*E-mail: kkadish@uh.edu.

Notes

The authors declare no competing financial interest.

ACKNOWLEDGMENTS

We gratefully acknowledge support from the Natural Science Foundation of China (No. 21071067, 21171076), the Robert A. Welch Foundation (K.M.K., Grant E-680), and National Science Foundation (V.N.N. CHE-1110455 and CHE-1401375).

REFERENCES

- (1) Nemykin, V. N.; Kobayashi, N. *Chem. Commun.* **2001**, 165–166.

- (2) Lukyanets, E. A.; Nemykin, V. N. *J. Porphyrins Phthalocyanines* **2010**, *14*, 1–40.
- (3) Nemykin, V. N.; Lukyanets, E. A. *ARKIVOC* **2010**, (i), 136–208.
- (4) An, M.; Kim, S.; Hong, J. D. *Bull. Korean Chem. Soc.* **2010**, *31*, 3272–3278.
- (5) Gonzalez-Cabello, A.; Claessens, C. G.; Martin-Fuch, G.; Ledoux-Rack, I.; Vazquez, P.; Zyss, J.; Agullo-Lopez, F.; Torres, T. *Synth. Met.* **2003**, *137*, 1487–1488.
- (6) Gonzalez-Cabello, A.; Vazquez, P.; Torres, T. *J. Organomet. Chem.* **2001**, 637–639, 751–756.
- (7) (a) Gryko, D. T.; Piechowska, J.; Jaworski, J. S.; Galezowski, M.; Tasiar, M.; Cembor, M.; Butenschoten, H. *New J. Chem.* **2007**, *31*, 1613–1619. (b) Pomarico, G.; Vecchi, A.; Mandoj, F.; Bortolini, O.; Cicero, D. O.; Galloni, P.; Paolesse, R. *Chem. Commun.* **2014**, *50*, 4076–4078.
- (8) Kumar, R.; Misra, R.; PrabhuRaja, V.; Chandrashekar, T. K. *Chem.—Eur. J.* **2005**, *11*, 5695–5707.
- (9) Venkatraman, S.; Kumar, R.; Sankar, J.; Chandrashekar, T. K.; Sendhil, K.; Vijayan, C.; Kelling, A.; Senge, M. O. *Chem.—Eur. J.* **2004**, *10*, 1423–1432.
- (10) Bucher, C.; Devillers, C. H.; Moutet, J. C.; Royal, G.; Saint-Aman, E. *Coord. Chem. Rev.* **2009**, *253*, 21–36.
- (11) Shoji, O.; Okada, S.; Satake, A.; Kobuke, Y. *J. Am. Chem. Soc.* **2005**, *127*, 2201–2210.
- (12) Shoji, O.; Tanaka, H.; Kawai, T.; Kobuke, Y. *J. Am. Chem. Soc.* **2005**, *127*, 8598–8599.
- (13) Auger, A.; Swarts, J. C. *Organometallics* **2007**, *26*, 102–109.
- (14) Nemykin, V. N.; Barrett, C. D.; Hadt, R. G.; Subbotin, R. I.; Maximov, A. Y.; Polshin, E. V.; Kuposov, A. Y. *Dalton Trans.* **2007**, 3378–3389.
- (15) Nemykin, V. N.; Galloni, P.; Floris, B.; Barrett, C. D.; Hadt, R. G.; Subbotin, R. I.; Marrani, A. G.; Zaroni, R.; Loim, N. M. *Dalton Trans.* **2008**, 4233–4246.
- (16) Nemykin, V. N.; Rohde, G. T.; Barrett, C. D.; Hadt, R. G.; Bizzarri, C.; Galloni, P.; Floris, B.; Nowik, I.; Herber, R. H.; Marrani, A. G.; Zaroni, R.; Loim, N. M. *J. Am. Chem. Soc.* **2009**, *131*, 14969–14978.
- (17) Nemykin, V. N.; Rohde, G. T.; Barrett, C. D.; Hadt, R. G.; Sabin, J. R.; Reina, G.; Galloni, P.; Floris, B. *Inorg. Chem.* **2010**, *49*, 7497–7509.
- (18) Rohde, G. T.; Sabin, J. R.; Barrett, C. D.; Nemykin, V. N. *New J. Chem.* **2011**, *35*, 1440–1448.
- (19) Solntsev, P. V.; Neisen, B. D.; Sabin, J. R.; Gerasimchuk, N. N.; Nemykin, V. N. *J. Porphyrins Phthalocyanines* **2011**, *15*, 612–621.
- (20) Kubo, M.; Mori, Y.; Otani, M.; Murakami, M.; Ishibashi, Y.; Yasuda, M.; Hosomizu, K.; Miyasaka, H.; Imahori, H.; Nakashima, S. *J. Phys. Chem. A* **2007**, *111*, 5136–5143.
- (21) Rochford, J.; Rooney, A. D.; Pryce, M. T. *Inorg. Chem.* **2007**, *46*, 7247–7249.
- (22) Galloni, P.; Floris, B.; de Cola, L.; Cecchetto, E.; Williams, R. M. *J. Phys. Chem. C* **2007**, *111*, 1517–1523.
- (23) Nemykin, V. N.; Hadt, R. G. *J. Phys. Chem. A* **2010**, *114*, 12062–12066.
- (24) Vecchi, A.; Gatto, E.; Floris, B.; Conte, V.; Venanzi, M.; Nemykin, V. N.; Galloni, P. *Chem. Commun.* **2012**, 48, 5145–5147.
- (25) Sharma, R.; Gautam, P.; Mobin, S. M.; Misra, R. *Dalton Trans.* **2013**, 42, 5539–5545.
- (26) Pareek, Y.; Ravikanth, M. *J. Organomet. Chem.* **2013**, *724*, 67–74.
- (27) Samanta, S.; Mitra, K.; Sengupta, K.; Chatterjee, S.; Dey, A. *Inorg. Chem.* **2013**, *52*, 1443–1453.
- (28) Devillers, C. H.; Milet, A.; Moutet, J.-C.; Pecaut, J.; Royal, G.; Saint-Aman, E.; Bucher, C. *Dalton Trans.* **2013**, 42, 1196–1209.
- (29) Osipova, E. Yu.; Rodionov, A. N.; Simenel, A. A.; Belousov, Y. A.; Nikitin, O. M.; Kachala, V. V. *J. Porphyrins Phthalocyanines* **2012**, *16*, 1225–1232.
- (30) Nemykin, V. N.; Chen, P.; Solntsev, P. V.; Purchel, A. A.; Kadish, K. M. *J. Porphyrins Phthalocyanines* **2012**, *16*, 793–801.
- (31) Bakar, M. A.; Sergeeva, N. N.; Juillard, T.; Senge, M. O. *Organometallics* **2011**, *30*, 3225–3228.
- (32) Lyons, D. M.; Mohanraj, J.; Accorsi, G.; Armaroli, N.; Boyd, P. D. W. *New J. Chem.* **2011**, *35*, 632–639.
- (33) Subbaiyan, N. K.; Wijesinghe, C. A.; D'Souza, F. J. *Am. Chem. Soc.* **2009**, *131*, 14646–14647.
- (34) Jiao, L.; Courtney, B. H.; Fronczek, F. R.; Smith, K. M. *Tetrahedron Lett.* **2006**, *47*, 501–504.
- (35) Wang, H. J. H.; Jaquinod, L.; Olmstead, M. M.; Vicente, M. G. H.; Kadish, K. M.; Ou, Z.; Smith, K. M. *Inorg. Chem.* **2007**, *46*, 2898–2913.
- (36) Gryko, D. T.; Zhao, F.; Yasseri, A. A.; Roth, K. M.; Bocian, D. F.; Kuhr, W. G.; Lindsey, J. S. *J. Org. Chem.* **2000**, *65*, 7356–7362.
- (37) Cheng, K. L.; Li, H. W.; Ng, D. K. P. *J. Organomet. Chem.* **2004**, *689*, 1593–1598.
- (38) Muraoka, T.; Kinbara, K.; Aida, T. *Nature* **2006**, *440*, 512–515.
- (39) Solntsev, P. V.; Sabin, J. R.; Dammer, S. J.; Gerasimchuk, N. N.; Nemykin, V. N. *Chem. Commun.* **2010**, 46, 6581–6583.
- (40) Kadish, K. M.; Xu, Q. Y.; Barbe, J. M. *Inorg. Chem.* **1987**, *26*, 2565–2566.
- (41) Xu, Q. Y.; Barbe, J. M.; Kadish, K. M. *Inorg. Chem.* **1988**, *27*, 2373–2378.
- (42) Wasielewski, M. R. *Chem. Rev.* **1992**, *92*, 435–461.
- (43) Gust, D.; Moore, T. A.; Moore, A. L. *Acc. Chem. Res.* **1993**, *26*, 198–205.
- (44) Health, J. R.; Kuekes, P. J.; Snider, G. S.; Williams, R. S. *Science* **1998**, *280*, 1716–1721.
- (45) Chen, Y.; Jung, J.; Ohlberg, D.; Li, X.; Stewart, D. R.; Jeppesen, K. A.; Stoddart, J. F.; Williams, R. S. *Nanotechnology* **2003**, *14*, 462–468.
- (46) Beer, P. D.; Gale, P. A.; Chen, G. Z. *Coord. Chem. Rev.* **1999**, *185/186*, 3–36.
- (47) Bard, A. J. *Nature* **1995**, *374*, 13–13.
- (48) Matsushige, K.; Yamada, H.; Tada, H.; Horiuchi, T.; Chen, X. Q. *Ann. N.Y. Acad. Sci.* **1998**, *852*, 290–305.
- (49) Liu, Z.; Yasseri, A. A.; Lindsey, J. S.; Bocian, D. F. *Science* **2003**, *302*, 1543–1545.
- (50) Kadish, K. M.; Van Caemelbecke, E.; Royal, G. In *The Porphyrin Handbook*; Kadish, K. M., Smith, K. M., Guillard, R., Eds.; Academic Press: New York, 2000; Vol. 8, Chapter 55, pp 1–144.
- (51) Zhu, J. L.; Zhang, X. F.; Fang, Y. Y.; Sun, B.; Lu, G. F.; Ou, Z. P. *Chin. J. Inorg. Chem.* **2013**, *29*, 199–205.
- (52) Dammer, S. J.; Solntsev, P. V.; Sabin, J. R.; Nemykin, V. N. *Inorg. Chem.* **2013**, *52*, 9496–9510.
- (53) Mase, K.; Ohkubo, K.; Fukuzumi, S. *J. Am. Chem. Soc.* **2013**, *135*, 2800–2808.
- (54) Fukuzumi, S.; Okamoto, K.; Gros, C. P.; Guillard, R. J. *Am. Chem. Soc.* **2004**, *126*, 10441–10449.
- (55) Das, D.; Lee, Y. M.; Ohkubo, K.; Nam, W.; Karlin, K. D.; Fukuzumi, S. *J. Am. Chem. Soc.* **2013**, *135*, 4018–4026.
- (56) Das, D.; Lee, Y. M.; Ohkubo, K.; Nam, W.; Karlin, K. D.; Fukuzumi, S. *J. Am. Chem. Soc.* **2013**, *135*, 2825–2834.
- (57) Fukuzumi, S.; Kotani, H.; Lucas, H. R.; Doi, K.; Suenobu, T.; Peterson, R. L.; Karlin, K. D. *J. Am. Chem. Soc.* **2010**, *132*, 6874–6875.
- (58) Sun, B.; Ou, Z. P.; Yang, S. B.; Meng, D. Y.; Lu, G. F.; Fang, Y. Y.; Kadish, K. M. *Dalton Trans.* **2014**, 43, 10809–10815.
- (59) Song, E.; Shi, C. N.; Anson, F. C. *Langmuir* **1998**, *14*, 4315–4321.
- (60) Conway, B. E.; Angerstein-Kozłowska, H.; Sharp, W. B. A.; Criddle, E. E. *Anal. Chem.* **1973**, *45*, 1331–1336.
- (61) Hsueh, K. L.; Gonzalez, E. R.; Srinivasan, S. *Electrochim. Acta* **1983**, *28*, 691–697.
- (62) Kadish, K. M.; Fremond, L.; Ou, Z. P.; Shao, J. P.; Shi, C. N.; Anson, F. C.; Burdet, F.; Gros, P. C.; Barbe, J. M.; Guillard, R. J. *Am. Chem. Soc.* **2005**, *127*, 5652–5631.
- (63) Shi, C. N.; Anson, F. C. *Inorg. Chem.* **1998**, *37*, 1037–1043.
- (64) Treimer, S.; Tang, A.; Johnson, D. C. *Electroanalysis* **2002**, *14*, 165–171.

(65) Adler, A. D.; Longo, F. R.; Kampas, F.; Kim, J. *J. Inorg. Nucl. Chem.* **1970**, *32*, 2443–2445.

(66) Zhu, W. H.; Sintic, M.; Ou, Z. P.; Sintic, P. J.; McDonald, J. A.; Brotherhood, P. R.; Crossley, M. J.; Kadish, K. M. *Inorg. Chem.* **2010**, *49*, 1027–1038.

(67) Boyd, P. D. W.; Burrell, A. K.; Campbell, W. M.; Cocks, P. A.; Gordon, K. C.; Jameson, G. B.; Officer, D. L.; Zhao, Z. *Chem. Commun.* **1999**, 637–638.

(68) (a) Mitra, K.; Chatterjee, S.; Samanta, S.; Dey, A. *Inorg. Chem.* **2013**, *52*, 14317–14325. (b) Sengupta, K.; Chatterjee, S.; Samanta, S.; Bandyopadhyay, S.; Dey, A. *Inorg. Chem.* **2013**, *52*, 2000–2014.

(69) Sullivan, M. G.; Kötz, R.; Haas, O. *J. Electrochem. Soc.* **2000**, *147*, 308–317.

(70) Sullivan, M. G.; Schnyder, B.; Bärtsch, M.; Allia, D.; Barbero, C.; Imhof, R.; Kötz, R. *J. Electrochem. Soc.* **2000**, *147*, 2636–2643.

(71) Yang, Y.; Lin, Z. G. *J. Appl. Electrochem.* **1995**, *25*, 259–266.

(72) Ou, Z. P.; Lü, A. X.; Meng, D. Y.; Shi, H.; Fang, Y. Y.; Lu, G. F.; Kadish, K. M. *Inorg. Chem.* **2012**, *51*, 8890–8896.

(73) Shi, C.; Steiger, B.; Yuasa, M.; Anson, F. C. *Inorg. Chem.* **1997**, *36*, 4294–4295.

(74) Bettelheim, A.; Chan, R. J. H.; Kuwana, T. *J. Electroanal. Chem.* **1979**, *99*, 391–397.